Characteristics and mixing state of amine-containing particles at a rural site in the Pearl River Delta, China.

Chunlei Cheng[1,2], Zuzhao Huang[3], Chak K. Chan[4], Yangxi Chu[4], Mei Li[1,2]*, Tao Zhang[5], Yubo Ou[5], Duohong Chen[5], Peng Cheng[1,2], Lei Li[1,2], Wei Gao[1,2], Zhengxu Huang[1,2], Bo Huang[1,2,6], Zhong Fu[6], Zhen Zhou[1,2]*

[1]Institute of Mass Spectrometer and Atmospheric Environment, Jinan University, Guangzhou 510632, China

[2]Guangdong Provincial Engineering Research Center for on-line source apportionment system of air pollution, Guangzhou 510632, China

[3]Guangzhou Environmental Technology Assessment Center, Guangzhou 510045, China

[4]School of Energy and Environment, City University of Hong Kong, Hong Kong, China

[5]State Environmental Protection Key Laboratory of Regional Air Quality Monitoring, Guangdong Environmental Monitoring Center, Guangzhou 510308, China

[6]Guangzhou Hexin Analytical Instrument Limited Company, Guangzhou 510530, China

Correspondence to: Mei Li (limei2007@163.com) and Zhen Zhou (zhouzhen@gig.ac.cn)

Tel: 86-20-85225991, Fax: 86-20-85225991

Abstract. Particulate amines play an important role for the particle acidity and hygroscopicity and also contribute to secondary organic aerosol mass. We investigated the sources and mixing states of particulate amines using a single-particle aerosol mass spectrometer (SPAMS) during summer and winter 2014 at a rural site in the Pearl River Delta, China. Amine-containing particles accounted for 11.1 % and 9.4 % of the total detected individual particles in summer and winter, respectively. Although the increase of amine-containing particle counts mostly occurred at night, no obvious correlations between amine-containing particles and ambient relative humidity (RH) were found during the sampling period. Among the three markers we considered, the most abundant amine marker was $^{74}(C_2H_5)_2NH_2^+$, which was detected in 90% and 86% of amine-containing particles in summer and winter, followed by amine marker ions of $^{59}(CH_3)_3N^+$, and $^{86}(C_2H_5)_2NCH_2^+$ which were detected in less than 10% of amine-containing particles during sampling period. The amine-containing particles were characterized by high fractions of carbonaceous marker ions, carbon-nitrogen fragments, sulfate and nitrate in both summer and winter. More than 90% of amine-containing particles were found to be internally mixed with sulfate throughout the sampling period, while the percentage of amine particles containing nitrate increased from 43% in summer to 69% in winter. Robust correlations between the peak intensities of amines and sulfate and nitrate were observed, suggesting the possible formation of aminium sulfate and nitrate salts. Interestingly, only 8% of amine particles contained ammonium in summer, while the percentage increased dramatically to 54 % in winter, indicating a relatively ammonium-poor state in summer and an ammonium-rich state in winter. The total ammonium-containing particles were investigated and showed a much lower abundance in ambient particles in summer (3.6%) than that in winter (32.6%), which suggests the ammonium-poor state of amine-containing particles in summer may be related to the lower abundance of ammonia/ammonium in gas and particle phase. In addition, higher abundance of amines in ammonium-containing particles than that of ammonium in amine-containing particles suggests a possible contribution of ammonium–amine exchange reactions to the low abundance of ammonium in amine-containing particles

at high ambient RH (72 ± 13 %) in summer. The particle acidity of amine-containing particles is estimated via the relative acidity ratio (R_a), which is defined as the ratio of the sum of the sulfate and nitrate peak areas divided by the ammonium peak area. The R_a was 326 ± 326 in summer and 31 ± 13 in winter, indicating that the amine-containing particles were more acidic in summer than in winter. However, after including amines along with the ammonium in the acidity calculation, the new R_a' values showed no seasonal change in summer (11 ± 4) and winter (10 ± 2), which suggests that amines could be a buffer for the particle acidity of ammonium-poor particles.

Keywords: Amine; Single particles; Mixing state; Aminium salts; Particle acidity; SPAMS.

1 Introduction

Amines, a group of nitrogen-containing organic compounds, are ubiquitous in the atmospheric gas and particle phases (Ge et al., 2011a). A variety of low molecular weight (LMW) aliphatic amines have been detected in emissions from anthropogenic and natural sources, including animal husbandry, biomass burning, industrial emissions, vehicle exhaust, and marine sources (Rogge et al., 1994;Rappert and Muller, 2005;Calderon et al., 2007;Ngwabie et al., 2007;Facchini et al., 2008;Ge et al., 2011a). LMW aliphatic amines have gas-phase concentrations two orders of magnitude lower than that of ammonia (NH_3) (Sorooshian et al., 2008), but are more alkaline than NH_3 (Ge et al., 2011b). Due to their strong basicity and water solubility, LMW amines can undergo acid-base reactions with sulfuric and nitric acid to form aminium salts (Angelino et al., 2001;Sorooshian et al., 2007;Pratt et al., 2009), which has been found to enhance new particle formation beyond the amounts produced from reactions between acids and NH_3 alone (Kurten et al., 2008;Berndt et al., 2010;Place et al., 2010;Wang et al., 2010). In addition, once partitioned into the particle phase, these LMW aliphatic amines can enhance aerosol particle hygroscopicity (Chu et al., 2015;Sauerwein et al., 2015). Furthermore, amines can be oxidized by OH radicals, NO_3 radicals, and O_3 in the atmosphere to form semi-volatile and non-volatile

102 compounds, some of which are highly toxic (Lee and Wexler, 2013), and which
103 contribute to secondary organic aerosol (SOA) mass (Murphy et al., 2007;Malloy et
104 al., 2009).

105   The mass concentration and temporal distribution of LMW aliphatic amines in
106 aerosols have been studied extensively in a variety of environments, and LMW
107 aliphatic amines account for 2–12 % of organic mass (Day et al., 2009;Gilardoni et al.,
108 2009;Liu et al., 2009;Russell et al., 2009;Williams et al., 2010). In recent years,
109 real-time single particle mass spectrometry has been used to measure the size and
110 chemical composition of individual amine-containing particles with high time
111 resolution. The mixing state and single-particle characteristics of amines have been
112 investigated in laboratory and field environments (Angelino et al., 2001;Moffet et al.,
113 2008;Silva et al., 2008;Pratt et al., 2009;Huang et al., 2012;Qin et al., 2012;Zhang et
114 al., 2012;Gaston et al., 2013;Zauscher et al., 2013). Pratt et al. (2009) studied seasonal
115 differences in aminium and ammonium salts on a single-particle basis using an
116 aerosol time-of-flight mass spectrometer (ATOFMS) coupled with a thermodenuder
117 and reported that the gas-to-particle partitioning of amines is dependent on particle
118 acidity. Healy et al. (2015) investigated the temporal distributions of alkylamines at
119 five European sites, and found that alkylamines were internally mixed with both
120 sulfate and nitrate, which suggests that the formation of aminium salts was important
121 at all sites. Zauscher et al. (2013) detected strong signals of amine marker
122 ($^{86}(C_2H_5)_2NCH_2^+$) in biomass burning aerosols associated with the increase of ambient
123 relative humidity, indicating the direct emission of amines from biomass burning and
124 the important influence of high RH (>90%) on the partitioning process of amines.
125 Huang et al. (2012) determined the mixing state of amine-containing particles in
126 Shanghai and found higher number concentrations of amine-containing particles in
127 winter than in summer, which they attributed to effective acid-base reactions between
128 sulfuric acid and amines under low-temperature, high-RH conditions. Zhang et al.
129 (2012) measured trimethylamine-containing particles in Guangzhou and found
130 preferential trimethylamine gas-to-particle partitioning during fog events. These field
131 observations emphasize the important role of acid-base reactions in the partitioning of

amines from the gas phase to the particle phase. Recent laboratory studies have revealed that the exchange between amine gases and particulate NH_3 and/or ammonium also contributes substantially to amine content and results in a depletion of NH_3 and/or ammonium in the particle phase (Lloyd et al., 2009;Bzdek et al., 2010;Qiu et al., 2011;Liu et al., 2012;Chan and Chan, 2013;Chu and Chan, 2016, 2017;Sauerwein and Chan, 2017); however, the significance of such exchange reactions in the ambient environment has not been fully explored. Therefore, the influence of ammonia and particle acidity on the distribution of amines in the particle phase should be studied comprehensively through field measurements.

The aim of this study was to investigate the mixing state of a series of LMW aliphatic amines with sulfate, nitrate, and ammonium in individual particles using a single-particle aerosol mass spectrometer (SPAMS) at a rural site in the Pearl River Delta, China. In order to explore amine origins and gas-to-particle partitioning processes, amine-containing particles from both summer and winter were classified into three types based on mass spectral patterns. The aminium sulfate and nitrate salt formation processes and internal mixing state with ammonium were used to deduce the relationship between amines and ammonium in the particle phase and the influence of amines on particle acidity.

2 Methods

2.1 Aerosol sampling

Ambient single particles were collected and analyzed using a SPAMS at the Guangdong Atmospheric Supersite (22.73° N, 112.93° E), a rural site in Heshan City in the Pearl River Delta (PRD), China (Figure S1). The sampling site is surrounded by villages and experiences little influence from local industrial emissions (Cheng et al., 2017). The SPAMS was installed at the top of the main building, and aerosols were introduced to the SPAMS through a 2.5 m copper tube and a silica gel drier. SPAMS sampling was conducted continuously from 18 July to 1 August 2014 and from 27 January to 8 February 2015; several hours of data are missing due to technical maintenance. During the sampling period, hourly O_3 concentrations were measured

161   using an O_3 analyzer (model 49i, Thermo Scientific). Meteorological data, including

162   temperature, relative humidity, wind speed, and wind direction, were also measured

163   during SPAMS sampling.

164   **2.2 SPAMS**

165   SPAMS was designed by the Guangzhou Hexin Analytical Company based on

166   preexisting ATOFMS principles (Prather et al., 1994;Noble and Prather, 1996). The

167   setup and design of the SPAMS has been detailed previously (Li et al., 2011). Briefly,

168   single particles are sampled through an 80 μm critical orifice into the aerodynamic

169   lens at a flow rate of 75 ml min^{-1}. Then, the particles pass consecutively through two

170   laser beams (diode Nd:YAG, 532 nm) spaced 6 cm apart, and the aerodynamic

171   diameter of the single particle is calculated using the particle flight time and velocity

172   between the two laser beams. The single particle velocity is also used to calculate the

173   precise time at which to fire the desorption and ionization laser (Nd:YAG laser,

174   266nm), which is positioned 12 cm downstream from the second laser beam. After

175   ionization, the positive and negative ions are detected by a Z-shaped bipolar

176   time-of-flight mass spectrometer. In this work, the ionization laser pulse energy was

177   0.6 mJ and the power density was 1.06×10^8 W cm^{-2} throughout the campaign. The

178   size range of single particles detected by SPAMS ranged from 0.2 to 2 μm, calibrated

179   with standard polystyrene latex spheres (Nanosphere size standards, Duke Scientific

180   Corp., Palo Alto) of 0.22–2.0 μm diameter before and after the campaign (Cheng et al.,

181   2017).

182   **2.3 Data analysis**

183   Particle size and chemical composition were obtained via SPAMS mass spectral

184   analysis using the Computational Continuation Core (COCO; version 3.0) toolkit in

185   Matlab. According to the field studies of ATOFMS and SPAMS, it is difficult to

186   accurately determine the number concentration of ambient particles using SPAMS

187   alone due to the size-dependent transmission efficiencies of particles through

188   aerodynamic lens and composition dependent matrix effect (Gross et al., 2000;Pratt

189   and Prather, 2012). Thus, the particle counts and size distributions presented in this

190   work should be interpreted as semi-quantitative and serve as a basis of comparison

analysis (Healy et al., 2012). Based on previous studies using ATOFMS and SPAMS instruments (Angelino et al., 2001;Huang et al., 2012;Qin et al., 2012;Zhang et al., 2012;Gaston et al., 2013;Zauscher et al., 2013;Healy et al., 2015), amine-containing particles were characterized by marker ions, including m/z $^{59}(CH_3)_3N^+$, $^{74}(C_2H_5)_2NH_2^+$, $^{86}(C_2H_5)_2NCH_2^+$, $^{101}(C_2H_5)_3N^+$, $^{102}(C_3H_7)_2NH_2^+$, and $^{143}(C_3H_7)_3N^+$ (Table 1). In this work, a particle was identified as amine-containing if it contained any of the marker ions listed above with a relative peak area (defined as the percentage contribution of the target ion peak area to the sum of all ion peak areas) greater than 1%. It should be noted that amine-containing particles are operationally defined and not exclusive, which also contained various chemical species in addition to amines. According to this criterion, 57452 and 68026 amine-containing particles were identified in summer and winter, respectively, which accounted for 11.1 % and 9.4 % of the total detected particles. These number fractions are consistent with previously reported observations in the PRD (Zhang et al., 2012). However, due to the absence of fog events during the campaign, no dramatic increases in amine-containing particles associated with high RH conditions (RH > 90 %) were observed. Marker ions of $^{59}(CH_3)_3N^+$, $^{74}(C_2H_5)_2NH_2^+$, $^{86}(C_2H_5)_2NCH_2^+$ were detected as the most abundant amines species during the sampling period, so particles containing each marker ion were selected to investigate the possible sources and characteristics of amine-containing particles. $^{30}CH_3NH^+$ is also an amine marker which has been reported by other single particle studies (Phares et al., 2003;Glagolenko and Phares, 2004). In this work the peak intensity of $^{30}CH_3NH^+$ was much lower compared with other amine markers, and all the particles containing $^{30}CH_3NH^+$ had strong signal of $^{74}(C_2H_5)_2NH_2^+$, so the $^{30}CH_3NH^+$-containing particles were not specifically discussed. An ion peak at m/z +46 was detected in the ambient single particles, which could be the amine marker of $^{46}(CH_3)_2NH_2^+$ and/or $^{46}Na_2^+$ according to reported studies (Guazzotti et al., 2001;Gaston et al., 2011;Healy et al., 2015). In this work the m/z +46-containing particles had no other amine markers as listed above, besides, these particles were enriched with sodium salts like $^{62}Na_2O^+$, $^{81}Na_2Cl^+$ and $^{147}Na(NO_3)_2^-$. Thus, m/z +46-containing particles were not classified as amine-containing particles and are

7

221 likely sea salts.

3 Results and Discussion

3.1 Seasonal variation of amine-containing particles

Spatial distributions of amine-containing particles associated with backward trajectories (48 hour) of air masses at 500m levels above the ground during the sampling period are shown in Figure 1. Cluster trajectories were calculated by MeteoInfo (Wang, 2014), and the box plots were conducted by Igor Pro-based program Histbox (Wu et al., 2018;Wu and Yu, 2018). In summer, high amine-containing particle counts were associated with air masses of Cluster 3 (41.67%) and Cluster 4 (30.06%) (Figure 1a) from continent and South China Sea separately, suggesting that the majority of amine-containing particles came from anthropogenic sources and coastal emissions. However, in winter, large amounts of amine-containing particles were associated with air masses of Cluster 4 (48.08%) (Figure 1b), indicating that amine-containing particles were related primarily with local emissions, such as animal husbandry, biomass burning, and vehicle exhaust. Anthropogenic emissions from Foshan and Guangzhou may also have contributed, as the sampling site is only 40 km and 56 km from these cities, respectively (Figure S1). Besides, the stagnant meteorological conditions associated with Cluster 4 also facilitated the partitioning of amines from gas to particle phase in winter.

The amine-containing particle count observed in summer (57452) was lower than it observed in winter (68026), but the abundance of amine-containing particles relative to the total particle count was higher in summer (11.1%) than in winter (9.4%). Temporal variations of total amine-containing particles and three amine marker ions are shown in Figure 2. The increase of amine-containing particles was mostly associated with high relative humidity (RH) at night in summer, while no direct connection between particle counts and RH was found in winter (Figure S2 a and b). High counts of amine-containing particles that extended in a few days were found from 22 to 24 July (in summer) and from 5 to 8 February (in winter). Among the three markers we considered, the most abundant amine marker was $^{74}(C_2H_5)_2NH_2^+$, which

250 was detected in 90% and 86% of amine-containing particles in summer and winter

251 (Table 2), followed by $^{59}(CH_3)_3N^+$ and $^{86}(C_2H_5)_2NCH_2^+$ which were detected in less

252 than 10% of amine-containing particles during sampling period. The amine particles

253 containing $^{74}(C_2H_5)_2NH_2^+$ and $^{86}(C_2H_5)_2NCH_2^+$ both exhibited a similar pattern with

254 total amine-containing particles suggesting a similar emission source of

255 $^{74}(C_2H_5)_2NH_2^+$ and $^{86}(C_2H_5)_2NCH_2^+$ (Figure 2). The temporal trend of

256 $^{59}(CH_3)_3N^+$-containing particles were different from those of $^{74}(C_2H_5)_2NH_2^+$ and

257 $^{86}(C_2H_5)_2NCH_2^+$; and the two sudden episodes of $^{59}(CH_3)_3N^+$ occurred from 27 to 29

258 July in summer were possibly due to the emission sources of trimethylamine (TMA).

259 The diurnal patterns of amine-containing particles are investigated in summer

260 and winter (Figure 3) and both showed higher counts at night. The small increase

261 from 6:00 to 9:00 LST throughout the campaign may have been due to local

262 emissions from vehicle exhaust (Cadle and Mulawa, 1980). Several field studies have

263 revealed the strong correlation between RH and particulate amines, suggesting that

264 high RH in fog events is favorable for the gas-to-particle partitioning of amines

265 (Jeong et al., 2011;Rehbein et al., 2011;Huang et al., 2012;Zhang et al., 2012). In this

266 work, although the increase of amine-containing particle counts mostly occurred at

267 night, no obvious correlations between diurnal amine-containing particles and RH

268 were found in summer (r^2=0.33) and winter (r^2=0.0003) (Figure S2). Although lower

269 temperature facilitates the partitioning of gaseous amines into the particulate phase

270 (Huang et al., 2012), no significant temperature differences were found both in

271 summer (day: 32±1.1 ℃; night: 27.5±1.1 ℃) and winter (day: 15±1.4 ℃; night:

272 13±0.8 ℃), which suggests a minor influence of temperature on the diurnal pattern of

273 amine-containing particles. The increase of amine-containing particles at night may be

274 influenced by particle acidity and emission sources of amines (Murphy et al.,

275 2007;Kurten et al., 2008;Silva et al., 2008).

3.2 Characteristics of amine-containing particles

277 The average mass spectra of amine-containing particles in summer and winter

278 are shown in Figure 4. The amine-containing particles were characterized by high

279 fractions of carbonaceous marker ions, including $^{27}C_2H_3^+$, $^{29}C_2H_5^+$, $^{36}C_3^+$, $^{37}C_3H^+$,

280 $^{43}C_2H_3O^+$, $^{48}C_4^+$, $^{51}C_4H_3^+$, $^{53}C_4H_5^+$, $^{60}C_5^+$, $^{63}C_5H_3^+$, $^{65}C_5H_5^+$, and $^{77}C_6H_5^+$; and amine

281 marker ions of $^{30}CH_3NH^+$, $^{59}(CH_3)_3N^+$, $^{74}(C_2H_5)_2NH_2^+$ and $^{86}(C_2H_5)_2NCH_2^+$ in the

282 positive mass spectrum in both summer and winter. The negative mass spectrum was

283 characterized by strong carbon-nitrogen fragments like $^{26}CN^-$ and $^{42}CNO^-$, as well as

284 abundant secondary ions of $^{46}NO_2^-$, $^{62}NO_3^-$, $^{80}SO_3^-$, and $^{97}HSO_4^-$ in both summer and

285 winter. In many field studies, aged carbonaceous particles always contain abundant

286 secondary ions of sulfate, nitrate, and ammonium. Interestingly, in this work, the

287 signals of $^{18}NH_4^+$ were weak and only observed in less than 10% of amine-containing

288 particles in summer, but moderate signal of $^{18}NH_4^+$ was detected in half of

289 amine-containing particles in winter. The low $^{18}NH_4^+$ signal in amine-containing

290 particles may have been due to the emission sources of ammonia and particle acidity,

291 which will be discussed in Section 3.3.

292   The unscaled size-resolved number distributions of total amine-containing

293 particles and amine particles containing three marker ions of $^{59}(CH_3)_3N^+$,

294 $^{74}(C_2H_5)_2NH_2^+$, and $^{86}(C_2H_5)_2NCH_2^+$ are shown in Figure 5. The amine-containing

295 particles exhibited unimodal distributions in the submicron mode from 0.4 to 1.5 μm

296 in both summer and winter, which may have resulted from gaseous amine

297 condensation on and/or reaction with fine mode particles from anthropogenic

298 emissions. Although amine-containing particles peaked at the size range of 0.5-0.7 μm

299 in both summer and winter, a broader size range of amine-containing particles was

300 observed in winter, which may be due to more complex anthropogenic emission

301 sources of primary particles in winter. The $^{74}(C_2H_5)_2NH_2^+$-containing particles showed

302 similar variation patterns as total amine-containing particles both in summer and

303 winter. However, $^{59}(CH_3)_3N^+$- and $^{86}(C_2H_5)_2NCH_2^+$-containing particles showed less

304 distinct peaks in winter.

305 **3.3 Mixing state of amine-containing particles**

306   To investigate the mixing state of amine-containing particles, the abundances of

307 sulfate-, nitrate-, and ammonium-containing amine particles are shown in Table 3.

308 More than 90% of amine-containing particles were found to be internally mixed with

309 sulfate throughout the sampling period. The abundance of nitrate in amine particles

310 increased from 43% in summer to 69% in winter. The internal mixing state of amines

311 with sulfate and nitrate had also been found in Qin et al. (2012), which reported that

312 the amine-rich particles consisted of $18\pm10\%$ amines by mass in the form of aminium

313 sulfate and nitrate salts in summer in Riverside, California. In this work, the high

314 abundances of sulfate and nitrate in amine-containing particles suggest the possible

315 formation of aminium sulfate and nitrate salts. Interestingly, only 8% of

316 amine-containing particles mixed with ammonium (NH_4^+) in summer, while the

317 percentage increased dramatically to 54 % in winter, indicating a relatively NH_4^+-poor

318 state in summer and an NH_4^+-rich state in winter.

319   The seasonal differences of the mixing state of amines and NH_4^+ may be

320 influenced by the seasonal variation of source strength of NH_4^+. To investigate the

321 temporal variation and abundance of NH_4^+ in total detected single particles, the total

322 NH_4^+-containing particles were identified with relative area of $^{18}NH_4^+$ larger than 1%.

323 Using this criterion, 18336 and 235312 of NH_4^+-containing particles were detected in

324 summer and winter separately, accounting for 3.6% and 32.6% of the total detected

325 particles. The averaged positive and negative ion mass spectra of NH_4^+-containing

326 particles are exhibited in Figure 6. During the entire sampling period the

327 NH_4^+-containing particles were characterized by abundant hydrocarbon fragments and

328 secondary organic species like $^{43}C_2H_3O^+$ and $^{89}HC_2O_4^-$, as well as strong signals of

329 $^{26}CN^-$, $^{42}CNO^-$, $^{62}NO_3^-$ and $^{97}HSO_4^-$, indicating an mixing state of NH_4^+-containing

330 particles. Also, 20% of NH_4^+-containing particles contained $^{74}(C_2H_5)_2NH_2^+$, which

331 indicates a close connection between NH_3 and diethylamine (DEA), possibly due to

332 the similar emission sources.

333   Temporal variations of total amine-containing particles, total

334 ammonium-containing (NH_4^+-containing) particles and particles containing both

335 ammonium and amine (NH_4^+-amine) are shown in Figure 7. The total

336 NH_4^+-containing particles and NH_4^+-amine particles were both much lower in summer

337 than in winter, and the NH_4^+-containing particles and amine-containing particles

338 showed a robust linear correlation in winter (r^2=0.63) (Figure S3). This seasonal

339 difference may be due to the low emission sources of ammonia and preferred

340   partitioning in gas phase in summer. Backward trajectories analysis (Figure 1) showed

341   that in summer the air mass was mainly from south of the sampling site and linked to

342   the marine region with low emission of anthropogenic pollutants. By contrast, in

343   winter, the air mass was mainly from northwest of the sampling site and associated

344   with relatively polluted megacities like Guangzhou and Foshan. In this work the lower

345   abundance of NH_4^+ was observed in summer (RH = 72 $\pm$ 13%) than in winter (RH

346   =63 $\pm$ 11%), suggesting a more important influence of sources than RH on the

347   seasonal trends of NH_4^+-containing particles.

348   The temporal variations of the peak areas of amines, ammonium, sulfate and

349   nitrate in amine-containing particles are shown in Figure 8. The peak areas of amines

350   and sulfate had similar variation patterns both in summer and winter, and the linear

351   regression between them showed robust correlations both in summer (r^2=0.69) and

352   winter (r^2=0.72) (Figure S4), indicating the formation of aminium sulfate salt during

353   the entire sampling period. However, the peak areas of amines and nitrate only

354   exhibited similar trends in winter, and the linear regression between them showed a

355   better correlation in winter (r^2=0.78) than in summer (r^2=0.52) (Figure S4), suggesting

356   the possible formation of aminium nitrate salt in winter. Low peak area of ammonium

357   was found in the amine-containing particles in summer which was in accordance with

358   the small amount of NH_4^+-amine particles. However, in winter, the peak area of

359   ammonium was comparable with amines and they both exhibited similar temporal

360   trends. In this work the particle acidity of amine-containing particles is represented by

361   the relative acidity ratio (R_a), which is developed by Denkenberger et al. (2007) and

362   Pratt et al. (2009), defined as the ratio of the sum of the sulfate and nitrate peak areas

363   divided by the ammonium peak area (Denkenberger et al., 2007;Pratt et al.,

364   2009;Cheng et al., 2017). Huang et al. (2013) obtained a robust correlation (r^2=0.82)

365   between the particle acidity calculated from inorganic ions obtained from MARGA

366   and relative acidity ratio obtained from single particle mass spectrometer, allowing us

367   to use R_a for comparison of particle acidity(Huang et al., 2013). The R_a was 326 $\pm$ 326

368   in summer and 31 $\pm$ 13 in winter (Figure 8), indicating that the amine-containing

369   particles were more acidic in summer than in winter.

370   Although high acidity promotes gaseous ammonia partitioning, extremely low
371   ammonium peak areas were found for the amine-containing particles in summer
372   (Figure 8), which may be associated with ammonium–amine exchange reactions in
373   addition to the low emission source of ammonia. The exchange between amine gases
374   and particulate NH_3 and/or ammonium highly depends on the RH and particle acidity
375   (Chan and Chan, 2013;Chu and Chan, 2016). According to the study of Sauerwein
376   and Chan, the co-uptake of dimethylamine (DMA) and ammonia (NH_3) by sulfuric
377   acid particles at 50% RH led to particle-phase dimethylaminium ($DMAH^+$) to
378   ammonium (NH_4^+) molar ratio up to four times that of gas-phase DMA to ammonia
379   molar ratio (0.1 and 0.5), suggesting the displacement of NH_4^+ by DMA during the
380   uptake process (Sauerwein and Chan, 2017). In this work, the ambient RH and acidic
381   particles containing abundant sulfate and nitrate were similar to the experimental
382   conditions used in Sauerwein and Chan (2017). In summer 8% of amine-containing
383   particles contained NH_4^+, while 25% of ammonium-containing particles contained
384   amines (Figure 7). Although the gas-phase concentrations of amines and NH_3 are not
385   quantified, higher abundance of amines in ammonium-containing particles than that of
386   ammonium in amine-containing particles suggests a possible ammonium–amine
387   exchange reactions in acidic particles in summer.

388   As strong bases, the presence of amines could have an impact on the particle
389   acidity. After including amines along with the ammonium in the relative acidity ratio
390   calculation, the new R_a' values (redefined as the ratio of the sum of the sulfate and
391   nitrate peak areas to the sum of the ammonium and amine peak areas) decrease to 11
392   ± 4 and 10 ± 2 in summer and winter, respectively, which are 30 and 3 times lower
393   than R_a values. R_a' showed no obvious seasonal change of particle acidity, which
394   suggests that amines could be a buffer for the particle acidity of ammonium-poor
395   particles, implying that it is reasonable to consider amines to calculate particle acidity
396   and actual pH.

397   **4 Summary and Conclusions**

398   Amine-containing particles were investigated using a single particle aerosol mass

399   spectrometer from 18 July to 1 August 2014, and from 27 January to 8 February 2015

400   in Heshan, China. Amine-containing particles accounted for 11.1 % and 9.4 % of the

401   total detected single particles in summer and winter, respectively; both seasons were

402   dominated by amine marker of $^{74}(C_2H_5)_2NH_2^+$ in 90% and 86% of amine-containing

403   particles in summer and winter, respectively. Amine markers of $^{59}(CH_3)_3N^+$ and

404     $^{86}(C_2H_5)_2NCH_2^+$ were detected in 4.5% and 5.5% of amine-containing particles in

405   summer, while their percentages both increased two times in winter. The amine

406   particles contained $^{74}(C_2H_5)_2NH_2^+$ and $^{86}(C_2H_5)_2NCH_2^+$ both exhibited similar

407   variation pattern with total amine-containing particles suggesting a similar emission

408   source of $^{74}(C_2H_5)_2NH_2^+$ and $^{86}(C_2H_5)_2NCH_2^+$, while the $^{59}(CH_3)_3N^+$-containing

409   particles showed different temporal trends, and two sudden increase episodes of

410     $^{59}(CH_3)_3N^+$ in summer was possibly due to the emission sources of trimethylamine.

411   Although the increase of amine-containing particle count mostly occurred at night, no

412   obvious correlations between amine-containing particles and RH were found in

413   summer (r^2=0.33) and winter (r^2=0.0003). More than 90% of amine-containing

414   particles contained strong signals of sulfate throughout the sampling period, while 43%

415   and 69% of amine particles contained nitrate in summer in winter. Only 8% of amine

416   particles contained ammonium in summer, while the percentage increased

417   dramatically to 54% in winter. Due to the lower percentage of total

418   ammonium-containing particles in summer (3.6%) than it in winter (32.6%), the

419   relatively ammonium-poor state of amine-containing particles in summer may be due

420   to the lower abundance of ammonia/ammonium in gas and particle phase. Besides, 8%

421   of amine-containing particles contained ammonium while 25% of

422   ammonium-containing particles contained amines in summer, suggesting a possible

423   contribution of ammonium–amine exchange reactions to the low abundance of

424   ammonium in amine-containing particles at high ambient RH (72 ± 13 %) in summer.

425   In addition, the presence of aminium salts affects the water activities and osmotic

426   coefficients of aqueous solutions, which may influence the calculation of pH using

427   aerosol thermodynamic models (Sauerwein et al., 2015). Furthermore, it should be

428   noted that the measured pH of bulk ambient aerosols may not be representative of the

actual single particle acidity. As pointed out in Pratt et al. (2009) and in this work, the mixing state of aerosols should be considered in order to comprehensively estimate the aerosol pH. Several recent studies have reported a 'missing' source of sulfate produced from the oxidation of SO_2 by NO_2 during haze episodes with high ambient relative humidity in northern China, and the neutralization of particulate ammonium is a key factor in this formation mechanism (Cheng et al., 2016;Wang et al., 2016). Our study reveals that amines have a potential influence on particle acidity, which could also impact this sulfate formation process during haze episodes. In order to discuss the potential role of amines in this sulfate formation pathway, real-time concentrations of amines, ammonium, sulfate, nitrate, and their precursors must be available. The results of this study suggest that amine chemistry involving particle acidity and mixing state with sulfate, nitrate and ammonium may have an important role in the aging process of particles in regions with high concentration of amines.

Author contributions: Chunlei Cheng and Mei Li designed the experiments. Tao Zhang, Yubo Ou and Duohong Chen carried them out. Chunlei Cheng prepared the manuscript with contributions from all co-authors.

Competing interests: Bo Huang and Zhong Fu are both employees at Guangzhou Hexin Analytical Instrument Limited Company.

References

467 Angelino, S., Suess, D. T., and Prather, K. A.: Formation of aerosol particles from
468   reactions of secondary and tertiary alkylamines: Characterization by aerosol
469   time-of-flight mass spectrometry, Environmental Science & Technology, 35,
470   3130-3138, 10.1021/es0015444, 2001.
471 Berndt, T., Stratmann, F., Sipila, M., Vanhanen, J., Petaja, T., Mikkila, J., Gruner, A.,
472   Spindler, G., Mauldin, R. L., Curtius, J., Kulmala, M., and Heintzenberg, J.:
473   Laboratory study on new particle formation from the reaction OH + SO2:
474   influence of experimental conditions, H2O vapour, NH3 and the amine
475   tert-butylamine on the overall process, Atmospheric Chemistry and Physics, 10,
476   7101-7116, 10.5194/acp-10-7101-2010, 2010.
477 Bzdek, B., Ridge, D., and Johnston, M.: Amine exchange into ammonium bisulfate
478   and ammonium nitrate nuclei, Atmospheric Chemistry and Physics, 10,
479   3495-3503, 2010.
480 Cadle, S. H., and Mulawa, P. A.: Low-molecular-weight aliphatic amines in exhaust
481   from catalyst-equipped cars, Environmental science & technology, 14, 718-723,
482   1980.
483 Calderon, S. M., Poor, N. D., and Campbell, S. W.: Estimation of the particle and gas
484   scavenging contributions to wet deposition of organic nitrogen, Atmospheric
485   Environment, 41, 4281-4290, 10.1016/j.atmosenv.2006.06.067, 2007.
486 Chan, L. P., and Chan, C. K.: Role of the Aerosol Phase State in Ammonia/Amines
487   Exchange Reactions, Environmental Science & Technology, 47, 5755-5762,
488   10.1021/es4004685, 2013.
489 Cheng, C., Li, M., Chan, C. K., Tong, H., Chen, C., Chen, D., Wu, D., Li, L., Wu, C.,
490   Cheng, P., Gao, W., Huang, Z., Li, X., Zhang, Z., Fu, Z., Bi, Y., and Zhou, Z.:
491   Mixing state of oxalic acid containing particles in the rural area of Pearl River
492   Delta, China: implications for the formation mechanism of oxalic acid,
493   Atmospheric Chemistry and Physics, 17, 9519-9533, 10.5194/acp-17-9519-2017,
494   2017.
495 Cheng, Y., Zheng, G., Wei, C., Mu, Q., Zheng, B., Wang, Z., Gao, M., Zhang, Q., He,

K., Carmichael, G., Pöschl, U., and Su, H.: Reactive nitrogen chemistry in aerosol water as a source of sulfate during haze events in China, Science Advances, 2, 10.1126/sciadv.1601530, 2016.

Chu, Y., and Chan, C. K.: Reactive Uptake of Dimethylamine by Ammonium Sulfate and Ammonium Sulfate–Sucrose Mixed Particles, The Journal of Physical Chemistry A, 121, 206-215, 10.1021/acs.jpca.6b10692, 2016.

Chu, Y., and Chan, C. K.: Role of oleic acid coating in the heterogeneous uptake of dimethylamine by ammonium sulfate particles, Aerosol Science and Technology, 51, 988-997, 10.1080/02786826.2017.1323072, 2017.

Chu, Y. X., Sauerwein, M., and Chan, C. K.: Hygroscopic and phase transition properties of alkyl aminium sulfates at low relative humidities, Phys Chem Chem Phys, 17, 19789-19796, 10.1039/c5cp02404h, 2015.

Day, D. A., Takahama, S., Gilardoni, S., and Russell, L. M.: Organic composition of single and submicron particles in different regions of western North America and the eastern Pacific during INTEX-B 2006, Atmospheric Chemistry and Physics, 9, 5433-5446, 2009.

Denkenberger, K. A., Moffet, R. C., Holecek, J. C., Rebotier, T. P., and Prather, K. A.: Real-time, single-particle measurements of oligomers in aged ambient aerosol particles, Environmental Science & Technology, 41, 5439-5446, 10.1021/es070329l, 2007.

Facchini, M. C., Decesari, S., Rinaldi, M., Carbone, C., Finessi, E., Mircea, M., Fuzzi, S., Moretti, F., Tagliavini, E., Ceburnis, D., and O'Dowd, C. D.: Important Source of Marine Secondary Organic Aerosol from Biogenic Amines, Environmental Science & Technology, 42, 9116-9121, 10.1021/es8018385, 2008.

Gaston, C. J., Furutani, H., Guazzotti, S. A., Coffee, K. R., Bates, T. S., Quinn, P. K., Aluwihare, L. I., Mitchell, B. G., and Prather, K. A.: Unique ocean‐derived particles serve as a proxy for changes in ocean chemistry, Journal of Geophysical Research: Atmospheres (1984–2012), 116, 10.1029/2010JD015289, 2011.

Gaston, C. J., Quinn, P. K., Bates, T. S., Gilman, J. B., Bon, D. M., Kuster, W. C., and Prather, K. A.: The impact of shipping, agricultural, and urban emissions on single particle chemistry observed aboard the R/V Atlantis during CalNex, Journal of Geophysical Research-Atmospheres, 118, 5003-5017, 10.1002/jgrd.50427, 2013.

Ge, X. L., Wexler, A. S., and Clegg, S. L.: Atmospheric amines - Part I. A review, Atmospheric Environment, 45, 524-546, DOI 10.1016/j.atmosenv.2010.10.012, 2011a.

Ge, X. L., Wexler, A. S., and Clegg, S. L.: Atmospheric amines - Part II. Thermodynamic properties and gas/particle partitioning, Atmospheric Environment, 45, 561-577, 10.1016/j.atmosenv.2010.10.013, 2011b.

Gilardoni, S., Liu, S., Takahama, S., Russell, L. M., Allan, J. D., Steinbrecher, R., Jimenez, J. L., De Carlo, P. F., Dunlea, E. J., and Baumgardner, D.: Characterization of organic ambient aerosol during MIRAGE 2006 on three platforms, Atmospheric Chemistry and Physics, 9, 5417-5432, 2009.

Glagolenko, S., and Phares, D. J.: Single-particle analysis of ultrafine aerosol in

College Station, Texas, Journal of Geophysical Research-Atmospheres, 109, 10.1029/2004jd004621, 2004.

Gross, D. S., Galli, M. E., Silva, P. J., and Prather, K. A.: Relative sensitivity factors for alkali metal and ammonium cations in single particle aerosol time-of-flight mass spectra, Anal. Chem., 72, 416-422, Doi 10.1021/Ac990434g, 2000.

Guazzotti, S. A., Whiteaker, J. R., Suess, D., Coffee, K. R., and Prather, K. A.: Real-time measurements of the chemical composition of size-resolved particles during a Santa Ana wind episode, California USA, Atmospheric Environment, 35, 3229-3240, 2001.

Healy, R., Sciare, J., Poulain, L., Kamili, K., Merkel, M., Müller, T., Wiedensohler, A., Eckhardt, S., Stohl, A., and Sarda-Estève, R.: Sources and mixing state of size-resolved elemental carbon particles in a European megacity: Paris, Atmospheric Chemistry and Physics, 12, 1681-1700, 2012.

Healy, R. M., Evans, G. J., Murphy, M., Sierau, B., Arndt, J., McGillicuddy, E., O'Connor, I. P., Sodeau, J. R., and Wenger, J. C.: Single-particle speciation of alkylamines in ambient aerosol at five European sites, Analytical and Bioanalytical Chemistry, 407, 5899-5909, 10.1007/s00216-014-8092-1, 2015.

Huang, Y., Chen, H., Wang, L., Yang, X., and Chen, J.: Single particle analysis of amines in ambient aerosol in Shanghai, Environmental Chemistry, 9, 202-210, 10.1071/EN11145, 2012.

Huang, Y., Li, L., Li, J., Wang, X., Chen, H., Chen, J., Yang, X., Gross, D. S., Wang, H., Qiao, L., and Chen, C.: A case study of the highly time-resolved evolution of aerosol chemical and optical properties in urban Shanghai, China, Atmospheric Chemistry and Physics, 13, 3931-3944, 10.5194/acp-13-3931-2013, 2013.

Jeong, C. H., McGuire, M. L., Godri, K. J., Slowik, J. G., Rehbein, P. J. G., and Evans, G. J.: Quantification of aerosol chemical composition using continuous single particle measurements, Atmospheric Chemistry and Physics, 11, 7027-7044, 10.5194/acp-11-7027-2011, 2011.

Kurten, T., Loukonen, V., Vehkamaki, H., and Kulmala, M.: Amines are likely to enhance neutral and ion-induced sulfuric acid-water nucleation in the atmosphere more effectively than ammonia, Atmospheric Chemistry and Physics, 8, 4095-4103, 2008.

Lee, D., and Wexler, A. S.: Atmospheric amines - Part III: Photochemistry and toxicity, Atmospheric Environment, 71, 95-103, DOI 10.1016/j.atmosenv.2013.01.058, 2013.

Li, L., Huang, Z. X., Dong, J. G., Li, M., Gao, W., Nian, H. Q., Fu, Z., Zhang, G. H., Bi, X. H., Cheng, P., and Zhou, Z.: Real time bipolar time-of-flight mass spectrometer for analyzing single aerosol particles, Int J Mass Spectrom, 303, 118-124, 10.1016/j.ijms.2011.01.017, 2011.

Liu, S., Takahama, S., Russell, L. M., Gilardoni, S., and Baumgardner, D.: Oxygenated organic functional groups and their sources in single and submicron organic particles in MILAGRO 2006 campaign, Atmospheric Chemistry and Physics, 9, 6849-6863, 2009.

Liu, Y., Han, C., Liu, C., Ma, J., Ma, Q., and He, H.: Differences in the reactivity of

ammonium salts with methylamine, Atmospheric Chemistry and Physics, 12, 4855-4865, 2012.

Lloyd, J. A., Heaton, K. J., and Johnston, M. V.: Reactive uptake of trimethylamine into ammonium nitrate particles, The Journal of Physical Chemistry A, 113, 4840-4843, 10.1021/jp900634d, 2009.

Malloy, Q. G. J., Li, Q., Warren, B., Cocker Iii, D. R., Erupe, M. E., and Silva, P. J.: Secondary organic aerosol formation from primary aliphatic amines with NO3 radical, Atmos. Chem. Phys., 9, 2051-2060, 10.5194/acp-9-2051-2009, 2009.

Moffet, R. C., de Foy, B., Molina, L. T., Molina, M. J., and Prather, K. A.: Measurement of ambient aerosols in northern Mexico City by single particle mass spectrometry, Atmospheric Chemistry and Physics, 8, 4499-4516, 10.5194/acp-8-4499-2008, 2008.

Murphy, S. M., Sorooshian, A., Kroll, J. H., Ng, N. L., Chhabra, P., Tong, C., Surratt, J. D., Knipping, E., Flagan, R. C., and Seinfeld, J. H.: Secondary aerosol formation from atmospheric reactions of aliphatic amines, Atmospheric Chemistry and Physics, 7, 2313-2337, 2007.

Ngwabie, N. M., Schade, G. W., Custer, T. G., Linke, S., and Hinz, T.: Volatile organic compound emission and other trace gases from selected animal buildings, Landbauforsch Volk, 57, 273-284, 2007.

Noble, C. A., and Prather, K. A.: Real-time measurement of correlated size and composition profiles of individual atmospheric aerosol particles, Environmental science & technology, 30, 2667-2680, 1996.

Phares, D. J., Rhoads, K. P., Johnston, M. V., and Wexler, A. S.: Size-resolved ultrafine particle composition analysis - 2. Houston, Journal of Geophysical Research-Atmospheres, 108, 10.1029/2001jd001212, 2003.

Place, P. F., Ziemba, L. D., and Griffin, R. J.: Observations of nucleation-mode particle events and size distributions at a rural New England site, Atmospheric Environment, 44, 88-94, 10.1016/j.atmosenv.2009.09.030, 2010.

Prather, K. A., Nordmeyer, T., and Salt, K.: Real-time characterization of individual aerosol particles using time-of-flight mass spectrometry, Anal. Chem., 66, 1403-1407, 1994.

Pratt, K. A., Hatch, L. E., and Prather, K. A.: Seasonal Volatility Dependence of Ambient Particle Phase Amines, Environmental Science & Technology, 43, 5276-5281, 10.1021/es803189n, 2009.

Pratt, K. A., and Prather, K. A.: Mass spectrometry of atmospheric aerosols—Recent developments and applications. Part II: On‐line mass spectrometry techniques, Mass Spectrom Rev, 31, 17-48, 2012.

Qin, X. Y., Pratt, K. A., Shields, L. G., Toner, S. M., and Prather, K. A.: Seasonal comparisons of single-particle chemical mixing state in Riverside, CA, Atmospheric Environment, 59, 587-596, 10.1016/j.atmosenv.2012.05.032, 2012.

Qiu, C., Wang, L., Lal, V., Khalizov, A. F., and Zhang, R.: Heterogeneous reactions of alkylamines with ammonium sulfate and ammonium bisulfate, Environmental science & technology, 45, 4748-4755, 2011.

Rappert, S., and Muller, R.: Odor compounds in waste gas emissions from agricultural

operations and food industries, Waste Manage, 25, 887-907, 10.1016/j.wasman.2005.07.008, 2005.

Rehbein, P. J. G., Jeong, C. H., McGuire, M. L., Yao, X. H., Corbin, J. C., and Evans, G. J.: Cloud and Fog Processing Enhanced Gas-to-Particle Partitioning of Trimethylamine, Environmental Science & Technology, 45, 4346-4352, 10.1021/es1042113, 2011.

Rogge, W. F., Hildemann, L. M., Mazurek, M. A., and Cass, G. R.: Sources of Fine Organic Aerosol .6. Cigarette-Smoke in the Urban Atmosphere, Environmental Science & Technology, 28, 1375-1388, 10.1021/Es00056a030, 1994.

Russell, L. M., Takahama, S., Liu, S., Hawkins, L. N., Covert, D. S., Quinn, P. K., and Bates, T. S.: Oxygenated fraction and mass of organic aerosol from direct emission and atmospheric processing measured on the R/V Ronald Brown during TEXAQS/GoMACCS 2006, Journal of Geophysical Research-Atmospheres, 114, 10.1029/2008jd011275, 2009.

Sauerwein, M., Clegg, S. L., and Chan, C. K.: Water Activities and Osmotic Coefficients of Aqueous Solutions of Five Alkylaminium Sulfates and Their Mixtures with H2SO4 at 25(o)C, Aerosol Science and Technology, 49, 566-579, 10.1080/02786826.2015.1043045, 2015.

Sauerwein, M., and Chan, C. K.: Heterogeneous uptake of ammonia and dimethylamine into sulfuric and oxalic acid particles, Atmos. Chem. Phys., 17, 6323-6339, 10.5194/acp-17-6323-2017, 2017.

Silva, P. J., Erupe, M. E., Price, D., Elias, J., Malloy, Q. G. J., Li, Q., Warren, B., and Cocker, D. R.: Trimethylamine as precursor to secondary organic aerosol formation via nitrate radical reaction in the atmosphere, Environmental Science & Technology, 42, 4689-4696, Doi 10.1021/Es703016v, 2008.

Sorooshian, A., Ng, N. L., Chan, A. W. H., Feingold, G., Flagan, R. C., and Seinfeld, J. H.: Particulate organic acids and overall water-soluble aerosol composition measurements from the 2006 Gulf of Mexico Atmospheric Composition and Climate Study (GoMACCS), Journal of Geophysical Research-Atmospheres, 112, 10.1029/2007jd008537, 2007.

Sorooshian, A., Murphy, S. N., Hersey, S., Gates, H., Padro, L. T., Nenes, A., Brechtel, F. J., Jonsson, H., Flagan, R. C., and Seinfeld, J. H.: Comprehensive airborne characterization of aerosol from a major bovine source, Atmospheric Chemistry and Physics, 8, 5489-5520, 2008.

Wang, G., Zhang, R., Gomez, M. E., Yang, L., Levy Zamora, M., Hu, M., Lin, Y., Peng, J., Guo, S., Meng, J., Li, J., Cheng, C., Hu, T., Ren, Y., Wang, Y., Gao, J., Cao, J., An, Z., Zhou, W., Li, G., Wang, J., Tian, P., Marrero-Ortiz, W., Secrest, J., Du, Z., Zheng, J., Shang, D., Zeng, L., Shao, M., Wang, W., Huang, Y., Wang, Y., Zhu, Y., Li, Y., Hu, J., Pan, B., Cai, L., Cheng, Y., Ji, Y., Zhang, F., Rosenfeld, D., Liss, P. S., Duce, R. A., Kolb, C. E., and Molina, M. J.: Persistent sulfate formation from London Fog to Chinese haze, Proceedings of the National Academy of Sciences, 113, 13630-13635, 10.1073/pnas.1616540113, 2016.

Wang, L., Khalizov, A. F., Zheng, J., Xu, W., Ma, Y., Lal, V., and Zhang, R. Y.: Atmospheric nanoparticles formed from heterogeneous reactions of organics, Nat

Geosci, 3, 238-242, 10.1038/NGEO778, 2010.

Wang, Y. Q.: MeteoInfo: GIS software for meteorological data visualization and analysis, Meteorol Appl, 21, 360-368, 10.1002/met.1345, 2014.

Williams, B. J., Goldstein, A. H., Kreisberg, N. M., Hering, S. V., Worsnop, D. R., Ulbrich, I. M., Docherty, K. S., and Jimenez, J. L.: Major components of atmospheric organic aerosol in southern California as determined by hourly measurements of source marker compounds, Atmospheric Chemistry and Physics, 10, 11577-11603, 10.5194/acp-10-11577-2010, 2010.

Wu, C., Wu, D., and Yu, J. Z.: Quantifying black carbon light absorption enhancement with a novel statistical approach, Atmospheric Chemistry and Physics, 18, 289-309, 10.5194/acp-18-289-2018, 2018.

Wu, C., and Yu, J. Z.: Evaluation of linear regression techniques for atmospheric applications: the importance of appropriate weighting, Atmos Meas Tech, 11, 1233-1250, 10.5194/amt-11-1233-2018, 2018.

Zauscher, M. D., Wang, Y., Moore, M. J. K., Gaston, C. J., and Prather, K. A.: Air Quality Impact and Physicochemical Aging of Biomass Burning Aerosols during the 2007 San Diego Wildfires, Environmental Science & Technology, 47, 7633-7643, 10.1021/es4004137, 2013.

Zhang, G., Bi, X., Chan, L. Y., Li, L., Wang, X., Feng, J., Sheng, G., Fu, J., Li, M., and Zhou, Z.: Enhanced trimethylamine-containing particles during fog events detected by single particle aerosol mass spectrometry in urban Guangzhou, China, Atmospheric Environment, 55, 121-126, 2012.

Tables and Figures

Table list:

Table 1. Marker ions chosen for the amine-containing particles

Table 2. Seasonal distributions of amine-containing particles and three major amine markers in summer and winter in the PRD, China.

Table 3. The abundances of ammonium-, nitrate- and sulfate-containing amine particles in total amine-containing particles.

Figure captions:

Figure 1. Spatial distributions of amine-containing particle counts associated with backward trajectories (48 hour) of air masses at 500m levels above the ground during the sampling period: (a) summer (from July 18 to August 1, 2014), (b) winter (from January 27 to February 8, 2015).

Figure 2. Temporal variations of relative humidity (RH), temperature (T), total amine-containing particles, and three major marker ions-containing amine particles ($^{59}(CH_3)_3N^+$, $^{74}(C_2H_5)_2NH_2^+$, $^{86}(C_2H_5)_2NCH_2^+$) in Heshan, China during sampling periods.

Figure 3. Diurnal variations of amine-containing particle counts in summer and winter in Heshan.

Figure 4. Average ion mass spectra of amine-containing particles in summer and winter. The color bars represent each peak area corresponding to a specific ion in individual particles.

Figure 5. Unscaled size-resolved number distributions of total amine-containing particles and amine particles containing three marker ions of $^{59}(CH_3)_3N^+$, $^{74}(C_2H_5)_2NH_2^+$, and $^{86}(C_2H_5)_2NCH_2^+$ in summer and winter in Heshan.

Figure 6. Mass spectra of total ammonium-containing (NH_4^+-containing) particles in summer and winter. The color bars represent each peak area corresponding to a specific fraction in individual particles.

Figure 7. Temporal variations of total amine-containing particles, total ammonium-containing particles, and particles containing both ammonium and amine (NH_4^+-amine) during sampling period in Heshan.

Figure 8. Temporal variations of the peak areas of amines, ammonium, sulfate and nitrate in amine-containing particles during summer and winter. The relative acidity

757   ratio (R_a), which was calculated as the ratio of the total sulfate and nitrate peak areas
758   to the ammonium peak area, is plotted as $\log(R_a)$.

Tables:

Table 1. Marker ions chosen for the amine-containing particles

Marker ion	Alkylamine assignment
$^{59}(CH_3)_3N^+$	Trimethylamine (TMA)[a]
$^{74}(C_2H_5)_2NH_2^+$	Diethylamine (DEA)[b]
$^{86}(C_2H_5)_2NCH_2^+$	DEA, TEA, DPA[c]
$^{101}(C_2H_5)_3N^+$	Triethylamine (TEA)[d]
$^{102}(C_3H_7)_2NH_2^+$	Dipropylamine (DPA)[e]
$^{143}(C_3H_7)_3N^+$	Tripropylamine (TPA)[f]

References are as follows: [a]Zhang et al., 2012, Gaston et al., 2013; [b]Angelino et al., 2001; [c]Huang et al., 2012, Zauscher et al., 2013, Qin et al., 2012; [d]Gaston et al., 2013; [e]Pratt et al., 2009; [f]Healy et al., 2015.

Table 2. Seasonal distributions of amine-containing particles and three major amine markers in summer and winter in the PRD, China.

Particle type	Summer (18/7-1/8, 2014)		Winter (27/1-8/2, 2015)	
	Count	Percentage (%)[a]	Count	Percentage (%)[a]
Total Amines	57452		68026	
$^{59}(CH_3)_3N^+$	2581	4.5	6894	10
$^{74}(C_2H_5)_2NH_2^+$	51442	90	58272	86
$^{86}(C_2H_5)_2NCH_2^+$	3185	5.5	6119	9

[a]The percentage of each amine marker ion in total detected amine-containing particles.

Table 3. The abundances of ammonium-, nitrate- and sulfate-containing amine particles in total amine-containing particles.

Marker ions	Summer	Winter
$^{18}NH_4^+$	8%	54%
$^{62}NO_3^-$	43%	69%
$^{97}HSO_4^-$	91%	94%

The marker ions of $^{18}NH_4^+$, $^{62}NO_3^-$ and $^{97}HSO_4^-$ were chosen to represent ammonium, nitrate and sulfate.
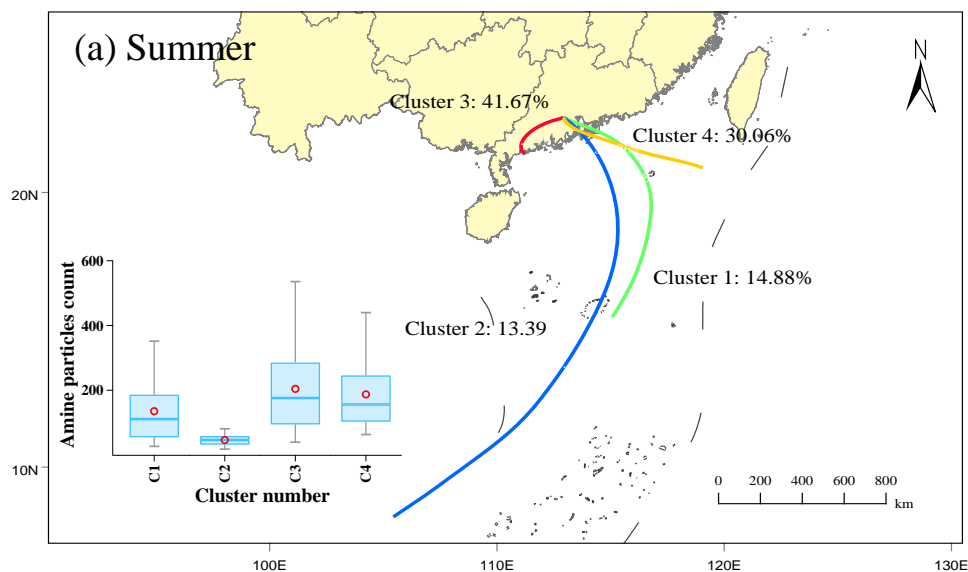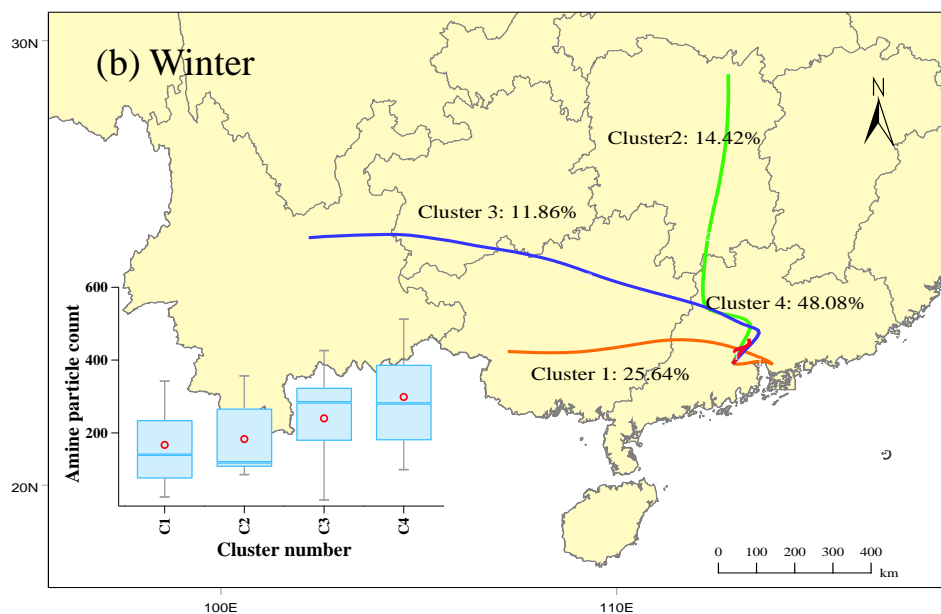
Figures:
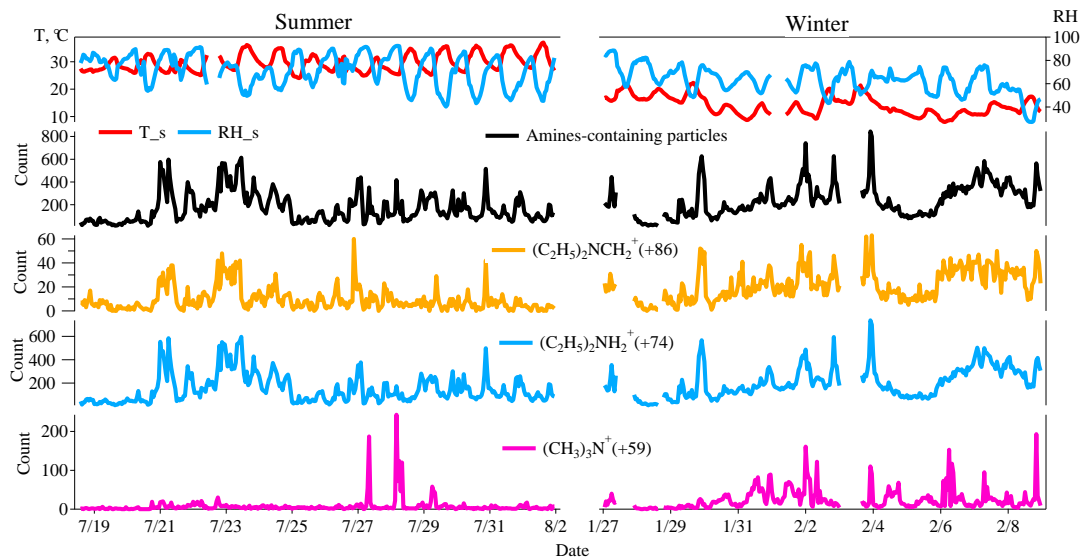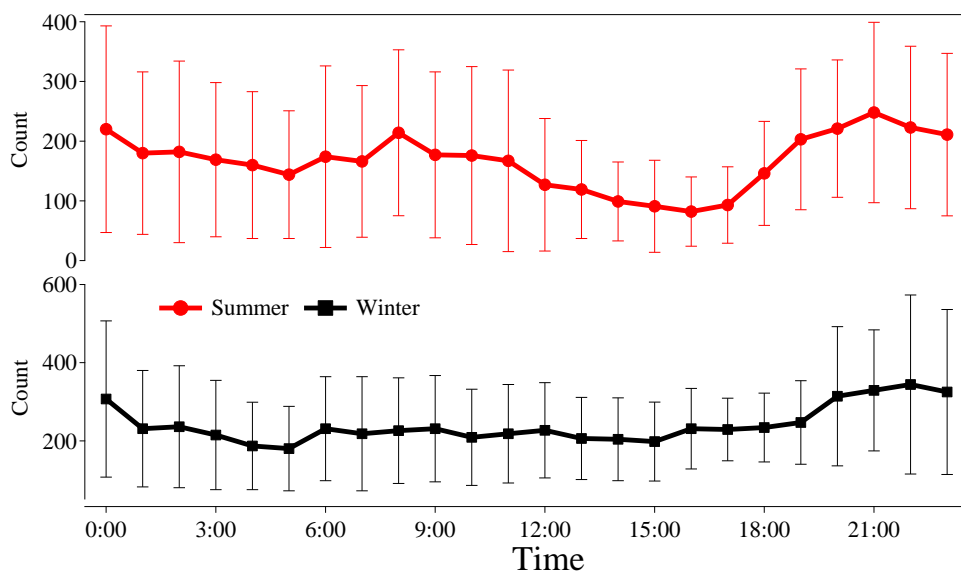
Figure 1. Spatial distributions of amine-containing particle counts associated with backward trajectories (48 hour) of air masses at 500m levels above the ground during the sampling period: (a) summer (from July 18 to August 1, 2014), (b) winter (from January 27 to February 8, 2015).
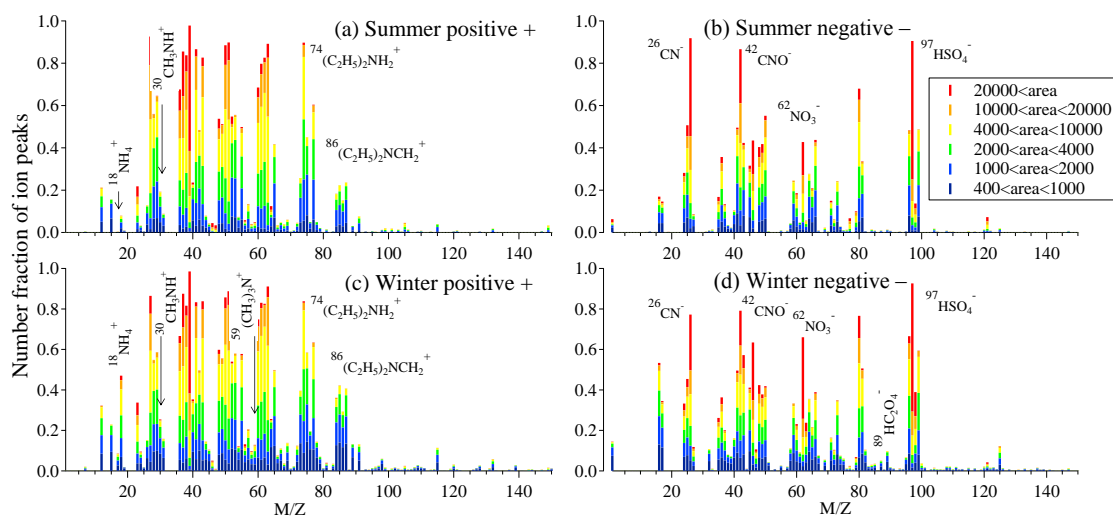
825

826 Figure 2. Temporal variations of relative humidity (RH), temperature (T), total
827 amine-containing particles, and three major marker ions-containing amine particles
828 ($^{59}(CH_3)_3N^+$, $^{74}(C_2H_5)_2NH_2^+$, $^{86}(C_2H_5)_2NCH_2^+$) in Heshan, China during sampling periods.

829

830

831

832

833

834 Figure 3. Diurnal variations of amine-containing particle counts in summer and winter
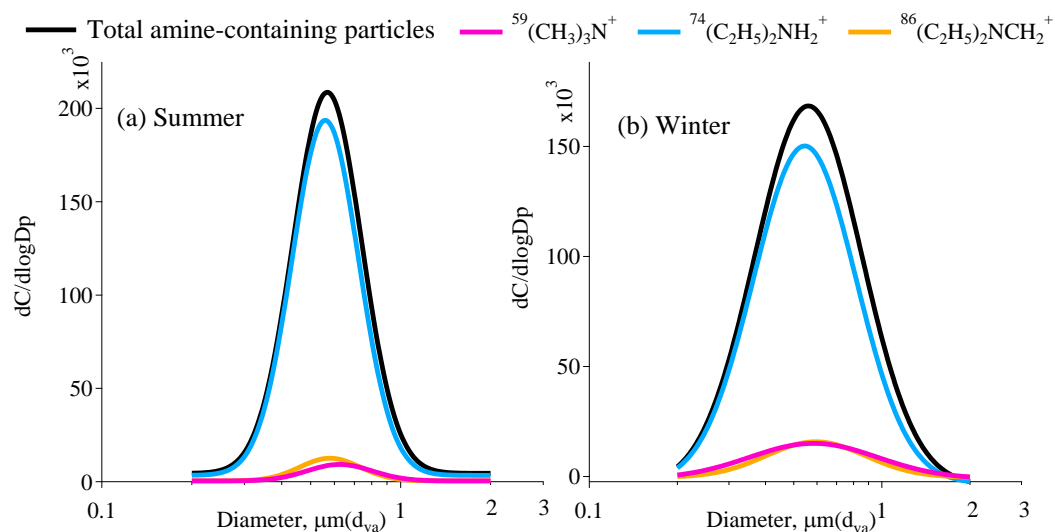835 in Heshan.

836

837

838

839

840

26

841

Figure 4. Average ion mass spectra of amine-containing particles in summer and winter. The color bars represent each peak area corresponding to a specific ion in individual particles.

Figure 5. Unscaled size-resolved number distributions of total amine-containing particles and amine particles containing three marker ions of $^{59}(CH_3)_3N^+$, $^{74}(C_2H_5)_2NH_2^+$, and $^{86}(C_2H_5)_2NCH_2^+$ in summer and winter in Heshan.
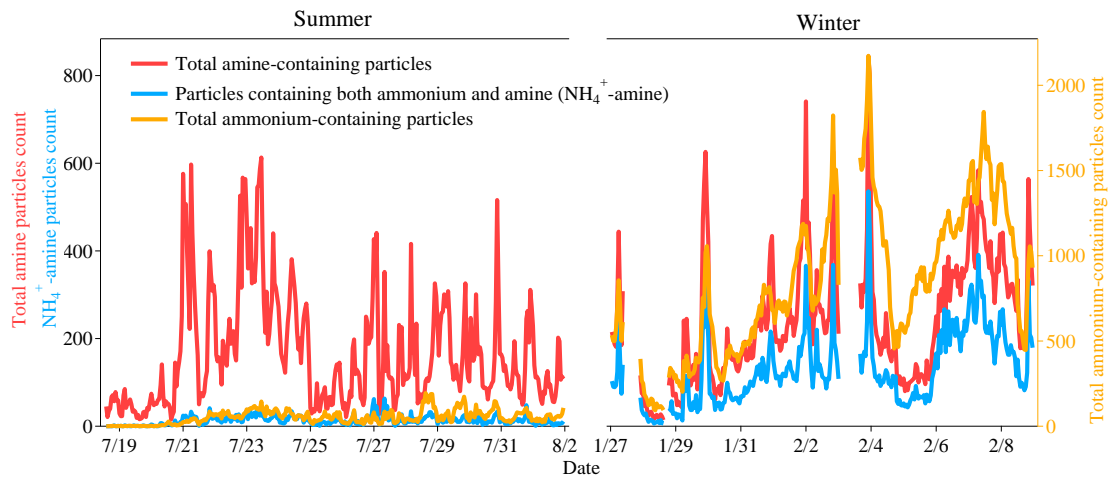
Figure 6. Mass spectra of total ammonium-containing (NH_4^+-containing) particles in summer and winter. The color bars represent each peak area corresponding to a specific fraction in individual particles.
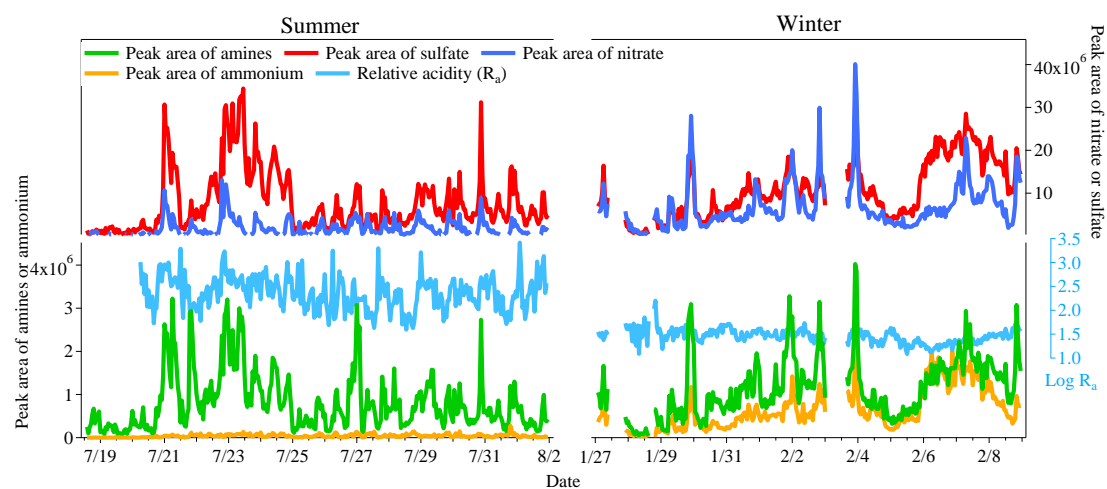
Figure 7. Temporal variations of total amine-containing particles, total ammonium-containing particles and particles containing both ammonium and amine (NH_4^+-amine) during sampling period in Heshan.

873
874
875
876
877
878
879

880

881

Figure 8. Temporal variations of the peak areas of amines, ammonium, sulfate and
nitrate in amine-containing particles during summer and winter. The relative acidity
ratio (R_a), which was calculated as the ratio of the total sulfate and nitrate peak areas
to the ammonium peak area, is plotted as $\log(R_a)$.

882
883
884
885
886